Materials Research Bulletin 48 (2013) 2614–2624

Contents lists available at SciVerse ScienceDirect

Materials Research Bulletin

journal homepage: www.elsevier.com/locate/matresbu

Synthesis of magnetite-porphyrin nanocomposite and its application as a novel magnetic adsorbent for removing heavy cations

Sara Bakhshayesh, Hossein Dehghani *

Department of Inorganic Chemistry, Faculty of Chemistry, University of Kashan, P.O. Box 87317-51167, Kashan, Iran

ARTICLE INFO

Article history:
Received 29 November 2012
Received in revised form 13 February 2013
Accepted 15 March 2013
Available online 25 March 2013

Keywords:
Nanocomposite
Magnetite
Porphyrin
Heavy cations
Adsorbent

ABSTRACT

Magnetite-porphyrin nanocomposite (MPNC) was synthesized as a novel magnetic adsorbent for removing heavy cations. Firstly, we prepared nano-sized magnetite using a simple hydrothermal route. The synthesis of nanoscaled magnetite was carried out through reaction between iron source and various amines. In this paper, we studied effective parameters in controlling shape and size of nanoscaled magnetite. These parameters were presence of alkaline, reaction time, kind of amine and iron salt. Morphology, particle size and magnetic properties of the nanoscaled magnetite were obtained by X-ray diffraction (XRD), scanning electron microscope (SEM), transmission electron microscope (TEM), Fourier transform infrared (FT-IR), diffuse reflectance spectra (DRS) and vibrating sample magnetometer (VSM). Our study showed that the synthesized magnetite from reaction between $FeSO_4$ and hydrazinum hydrate has spherical shape. The synthesized magnetite was a nanosized compound and used for preparation of magnetite-porphyrin nanocomposite. The synthesized magnetite-porphyrin hybrid material had magnetic property and was used as magnetic adsorbent for removing heavy cations of water. Satisfactory separation from solutions in the order of $Pb^{2+} > Cd^{2+} > Hg^{2+}$ was obtained.

1. Introduction

There is a very serious threat from the heavy metal pollution for the environment and all the life forms on the earth. This concern is because of rapid industrialization and increasing the world population. Research on heavy metal deposition and accumulation in the environment is the current attention of the most environmental scientists. The most studies focus on heavy metal concentrations in foods, vegetables, water, hematological parameters, atmosphere and soil [1,2]. Porphyrin derivatives play highly important roles in various fields of science, including chemistry, physics, geology, and biology. Researchers around the world have been studied porphyrins intensively from diverse viewpoints. The research conducted for many years proved versatility of porphyrin applications in the different areas of life [3]. The porphyrin derivatives can be used as sensitive indicator dyes for spectrophotometric determination of metal ions. There is an interest growing in the development of new sensing materials and the immobilization method to obtain sensors with improved characteristics. For example, it has been reported that porohyrin-silica hybrid material can be act as sensor for Ni^{2+}, Cu^{2+}, Pb^{2+} and Zn^{2+}ions [4].

Iron oxide nanostructures play an important role in science from technology to biotechnology. Iron oxides were widespread in nature. These compounds are ubiquitous in soils and sediments and have a profound influence on the water chemistry of aquifers and subsurface waters. Moreover, the formation of various iron oxides is dependent on abundance of water [5–7]. The iron oxides have been known for millennia. Such minerals were used originally as pigments for paints during the Paleolithic, since the uses of iron oxides have been expanded. Nowadays, iron oxides are used vastly in different fields; not only as pigments in paint but also as catalysts, sensors, recording media material and ferrofluids [8–17]. Magnetic nanoparticles have many unique magnetic properties such as supraparamagnetic, low Curie temperature, high magnetic susceptibility, high coercivity, etc. Magnetic nanoparticles are great interest to researchers in a wide range of fields, including magnetic fluids, data storage, catalysis, and biological applications such as MRI (magnetic resonance image) and targeted drug delivery. It has been reported various methods for synthesis and control of shape, size, stability and dispersibility of nanoparticles. For example, hydrothermal synthesis, thermal decomposition, co-precipitation, sol–gel processes, sonochemical synthesis and microemulsion methods have been reported in literature [18–25]. Magnetite is nonporous and its specific surface area ranges relative

* Corresponding author. Tel.: +98 361 591 2386; fax: +98 361 591 2397.
E-mail addresses: s_bakhshayesh@yahoo.com (S. Bakhshayesh), dehghani@kashanu.ac.ir (H. Dehghani).

0025-5408/$ – see front matter © 2013 Elsevier Ltd. All rights reserved.
http://dx.doi.org/10.1016/j.materresbull.2013.03.019

to preparation manner from is 4 $m^2 g^{-1}$to 100 $m^2 g^{-1}$ [5]. Due to their high surface area, iron oxides are used as sorbent for control the aqueous concentration of dissolved species, for example: arsenate, phosphate and heavy metals [26–31]. Magnetite (Fe_3O_4), as one of the basic magnetic materials has great potential for applications such as magnetic resonance imaging (MRI), magnetic bioseparation, magnetic drug targeting and gene delivery [32–36].

Magnetite is synthesized by hydrothermal decomposition of Fe^{II} or Fe^{III} chelates. The mixed oxides are more stable than pure Fe^{III} oxides [5]. There are some studies for synthesis of Fe_3O_4 nanoparticles with hydrothermal method. For example, Li et al. reported preparation of Fe_3O_4 nanoparticles at 150 °C in the presence of hydrazine [37]. Also, similar synthesis of magnetite nanoparticles has been reported by other researchers [38–45]. Using iron oxides for adsorption and recovery of metal ions from industrial waste or natural stream is an attractive subject. Magnetite separation method is a useful method for separation in solid-solid or liquid–solid phases. But there is aggregation problem due to interaction of magnetite particle with each other. Thus, providing a suitable surface coating to preserve the stability of magnetic iron oxide is very important. This coating can be done with small organic molecules, surfactants, polymers, and metal oxides or metal sulfide. Furthermore, in many cases, protecting shells not only to stabilize the magnetic iron oxide nanoparticles, but also can be used for further functionalization.

In attention to this background, we decided to synthesis of nanosized magnetite by a facile hydrothermal method, and so its application for preparation of magnetite-porphyrin nanocomposite. Furthermore, for the first time, we used the synthesized magnetite-porphyrin hybrid material as a magnetic adsorbent for removing heavy metals.

2. Experimental

2.1. Material

Chemicals for the synthesis of magnetite nanoparticles were $FeSO_4$, $FeCl_2$, $FeCl_3$, $Fe_2(SO_4)_3$, hydrazinum hydrate ($N_2H_4.H_2O$, 80%), 1,2-phenylenediamine (PDA), 1,8-naphthalenediamine (NDA) and NaOH that were purchased from Merck. The other used chemicals were ammonia, tetraethylorthosilicate (TEOS), ethanol, 4-methyl-4-(formylbenzoate) (96%), propionic acid, pyrrole (97%), nitrobenzene, tetrahydrofuran (THF), 3-aminopropyltrimethoxysilane (APTS) (98%), hydrochloric acid (32%), potassium hydroxide, N,N-dicyclohexylcarbodiimide (98%), triethylamine (98%), lead(II) nitrate, cadmium(II) nitrate, mercury(II) chloride. THF was dried and distilled over benzoic acid and sodium metal. Pyrrole was distilled before use too. Other chemicals were used as received and without additional purification. Deionized water was used throughout the experiments.

2.2. Physical measurements

X-ray diffraction (XRD) patterns were obtained on a Phillips X'Pert PRO with a Cu Kα radiation (λ = 1.54178 Å). The morphologies of the synthesized products were observed with a Philips XL-30ESEM scanning electron microscope (SEM). Fourier transform infrared (FT-IR) spectra were recorded with a Magna 550 Nicolet instrument (using KBr pellets). In addition, magnetic characterization of the samples was performed to measure the magnetic properties of them at room temperature by BHV-55, Riken, Japan vibrating sample magnetometer (VSM). The TEM image was obtained on a Zeiss EM10C transmission electron microscope with an accelerating voltage of 80 kV. Concentrations of Pb(II) and Cd(II) were determined using an atomic absorption spectrometer (Spectra AA 220, Varian) and the concentration of mercury ion was determined by UV–vis spectrophotometer (Spectronic 20D, Milton Roy Company). DRS spectra were obtained on a UV spectrophotometer 1800 Shimadzu within the wavelength 300–800 nm.

2.3. Methods

2.3.1. Synthesis of the nanosized magnetite

In a typical procedure, 1.0 mmol of $FeSO_4$ was dissolved in 5 ml of deionized water. Then, 5 ml of sodium hydroxide (0.4 M) was slowly dropped with steady stirring. Jadegreen colloid was immediately appeared in aqueous solution. The resulting mixture was stirred at room temperature for 10 min. Then, 0.18 ml $N_2H_4.H_2O$ (80%) was slowly added and the solution stirred for 10 min. The formed solution was transferred into a 25 ml autoclave. The autoclave was placed in an oven and kept at 150 °C for 15 h. At the end of the reaction, the product was cooled to room temperature, and the black precipitate was separated from solution and washed with distilled water and ethanol for several times. Then the obtained product was dried at 80 °C.

To study the effect of amine, all the reactions were repeated using PDA and NDA instead of hydrazinum hydrate. The effect of precursor was considered using $FeCl_2$, $FeCl_3$ and $Fe_2(SO_4)_3$ instead $FeSO_4$. The other factors were examined: the presence of NaOH, kind of amine and reaction time. Table 1 shows all synthesized samples under different conditions.

2.3.2. Synthesis of magnetite nanoparticles coated with silica (Fe_3O_4/SiO_2)

The magnetite nanoparticles coated with silica was synthesized by a reported method in the literature [46]. Firstly, the magnetite nanoparticles (0.1 g) were dispersed in a mixture of ethanol (10 ml) and deionized water (2 ml) by sonication for 10 min. After adding ammonia (0.25 ml) tetraethylorthosilicate (TEOS, 0.2 ml) was added to the reaction solution. The produced solution was stirred at room temperature. After 20 h, the magnetic product was collected and washed with ethanol and deionized water.

Table 1
Experimental parameters for the synthesized samples.

Sample	Precursor	Mineralizer	Temperature/°C	Time/h	Solvent
S1	$FeSO_4$	NaOH + $N_2H_4.H_2O$	150	4	H_2O
S2	$FeSO_4$	NaOH + $N_2H_4.H_2O$	150	12	H_2O
S3	$FeSO_4$	NaOH + $N_2H_4.H_2O$	150	15	H_2O
S4	$FeSO_4$	NaOH	150	15	H_2O
S5	$FeSO_4$	$N_2H_4.H_2O$	150	15	H_2O
S6	$Fe_2(SO_4)_3$	NaOH + $N_2H_4.H_2O$	150	15	H_2O
S7	$FeCl_2$	NaOH + $N_2H_4.H_2O$	150	15	H_2O
S8	$FeCl_3$	NaOH + $N_2H_4.H_2O$	150	15	H_2O
S9	$FeSO_4$	NaOH + PDA	150	15	H_2O
S10	$FeSO_4$	NaOH + NDA	150	15	H_2O
S11	$FeSO_4$	NaOH + $N_2H_4.H_2O$	150	15	C_2H_5OH

2.3.3. Synthesis of meso-tetrakis(4-carboxyphenyl)porphyrin

Porphyrin was synthesized according to the literature [47,48]. Freshly distilled pyrrole (1.42 ml, 20 mmol) and 3.42 g (20 mmol) of 4-methyl-4-(formylbenzoate) was added to a mixture of 15 ml nitrobenzene and 70 ml propionic acid. The solution was refluxed for 3.5 h, and was cooled to room temperature and filtered. The produced solid was washed with distilled water.

Meso-tetrakis(4-carboxymethylphenyl)porphyrin (0.085 g, 0.1 mmol) was dissolved in 100 ml of tetrahydrofuran (THF)-ethanol (1:1). Potassium hydroxide (0.513 g) in water (5 ml) was added and refluxed for 8 h. After cooling and removal of solvent, the residue was diluted with water (100 ml) and desired porphyrin tetrapotassium salt was filtered. Acidification (pH = 2) of an aqueous suspension of the porphyrin tetrapotassium salt with concentrated hydrochloric acid and subsequent filtration gave meso-tetrakis (4-carboxyphenyl)porphyrin as a purple powder. UV–vis (nm): 421.0, 514.5, 549.0, 590.1, 645.0, ^{1}H NMR (ppm): −2.98 (s, 2H, NH), 8.37 (s, 16H, o, m), 8.85(d, 8H, β), FT-IR (cm^{-1}): 1703, 3430

2.3.4. Modification of porphyrin and attachment to magnetic nanoparticles

Magnetite-porphyrin nanocomposite was obtained by modified method in the literature [49]. N,N-dicyclohexylcarbodiimide (0.18 g; 0.887 mmol) was added to a solution of Meso-tetrakis(4-carboxyphenyl)porphyrin (0.07 g; 0.0885 mmol) in dry THF (10 mL) and the reaction mixture was stirred for 3 h at 0 °C. To prevent any possible photobleaching of the porphryin, the reaction was carried out in the dark. 3-Aminopropyltrimethoxysilane (63 μl, 0.355 mmol) in 1 ml dry THF was added to the porphyrin solution at 0 °C. The reaction mixture was brought to room temperature and allowed to react overnight. The magnetite nanoparticles coated with silica (0.05 g) and triethylamine (300 μl) were added to the reaction vessel and allowed to react for 24 h. The mixture was centrifuged and the particles were washed with THF (5 × 10 ml) to remove any un-reacted porphyrin or unwanted side-products. The particles of magnetite-porphyrin nanocomposite (MPNC) were finally washed with water. Scheme 1 shows the schematic representation of the formation steps of magnetite-porphyrin nanocomposite (MPNC).

2.3.5. Investigation of magnetite-porphyrin nanocomposite (MPNC) as magnetic adsorbent for removing heavy cations

A known amount of MPNC was added to the 1 M solution of lead(II) nitrate in water. After 2 days, the solid phase was separated by magnetic separation. The concentration of lead in the sample was determined by atomic absorption method. The investigations of adsorption behavior of the MPNC for cadmium and mercury ion were repeated as mentioned above with solutions of cadmium(II) nitrate and mercury(II) chloride in water. The concentration of cadmium and mercury in the samples were determined by atomic absorption and dithizone methods, respectively [50]. Scheme 2 shows a schematic representation of the magnetic adsorbent for removal of heavy cations.

3. Results and discussion

The crystallinity and phase purity of the as-prepared products were examined by XRD measurements. Fig. 1 shows the XRD patterns of the obtained samples at various times for the reaction. As shown in this figure, the suitable time for the preparation of pure Fe_3O_4 is 15 h. For shorter times than 15 h, the product was not pure. The synthesized sample at 4 h (S1) was containing Fe_3O_4, Fe_2O_3 and FeS, and so the produced sample at 12 h (S2) was containing Fe_3O_4 and Fe_2O_3 as impurities. The XRD patterns of the obtained products in presence of NaOH (S4) and $N_2H_4.H_2O$ (S5) are shown in Fig. 2. This figure shows that S4 and S5 are not pure. The XRD patterns are shown that the S4 sample is containing impurities of Fe_2O_3 and FeOOH. Furthermore, the S5 is magnetite with impurities of Fe_2O_3 and $Fe(OH)_3$. Therefore, for preparation of

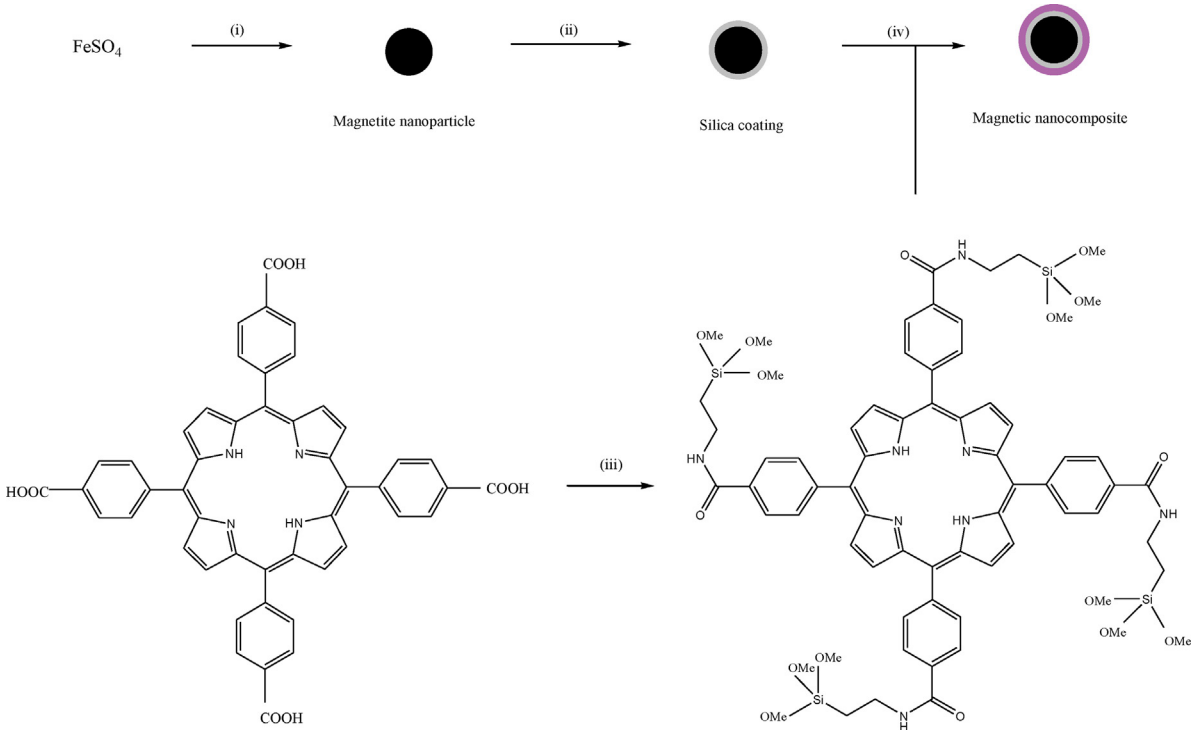

Scheme 1. Preparation of the MPNC: (i) magnetite nanoparticles is synthesized from $FeSO_4$ with $N_2H_4.OH$ (15 h, 150 °C) (ii) a thin silica layer is introduced on the magnetite nanoparticle surface by employing tetraorthosilicate (TEOS). (iii) an amide coupling reaction is performed between the carboxylic acid groups of porphyrin and 3-APTS. (iv) magnetite-porphyrin nanocomposite is result of a base hydrolysis between the modified porphyrin and the magnetite nanoparticles coated with silica.

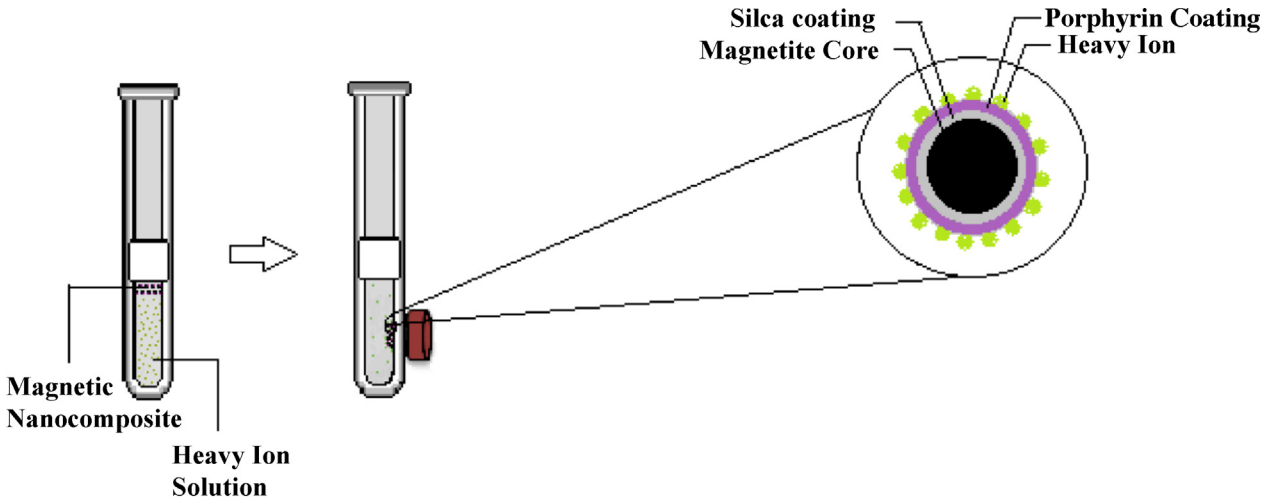

Scheme 2. Removing heavy ion from solution with magnetic adsorbent.

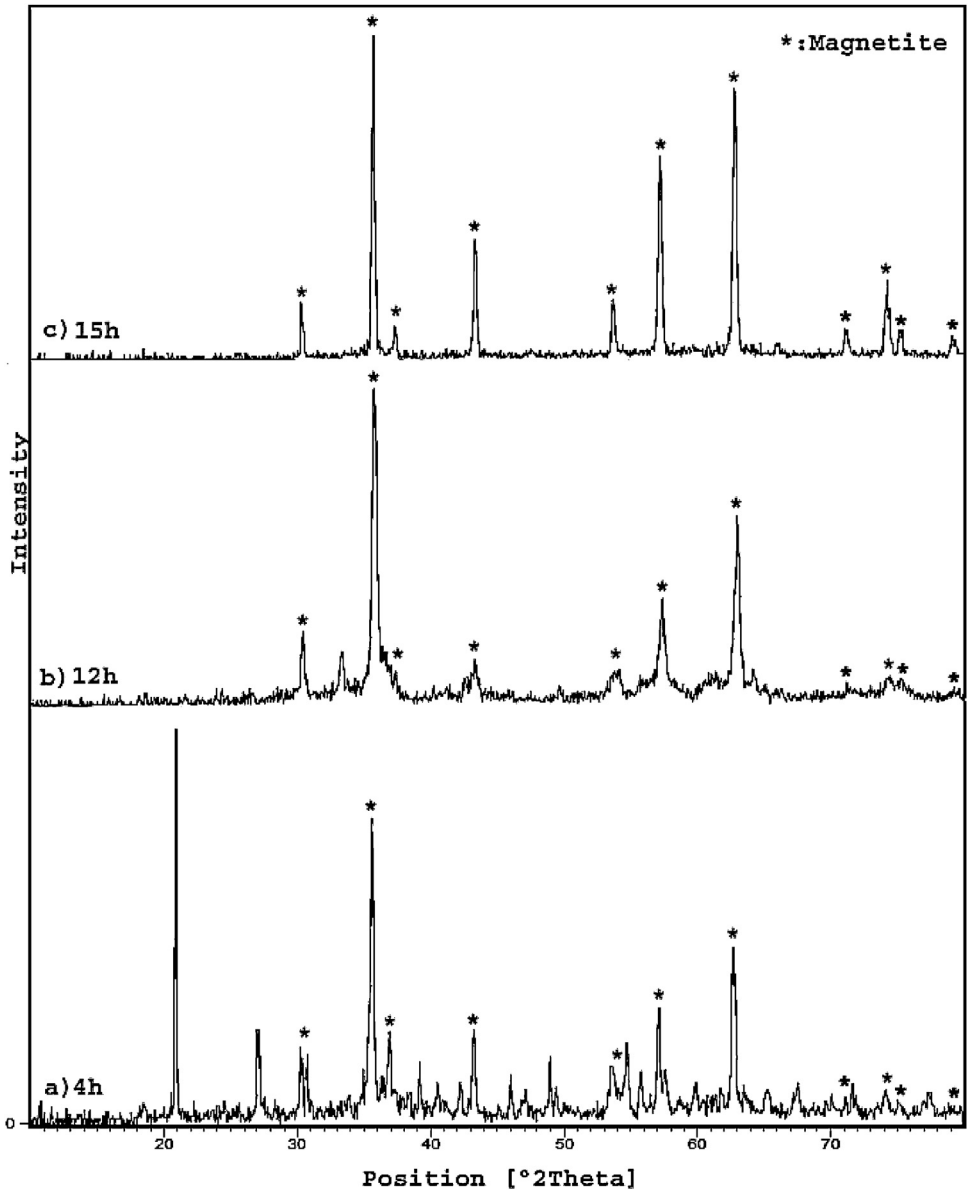

Fig. 1. XRD patterns of obtained samples at various times: (a) S1, (b) S2, and (c) S3.

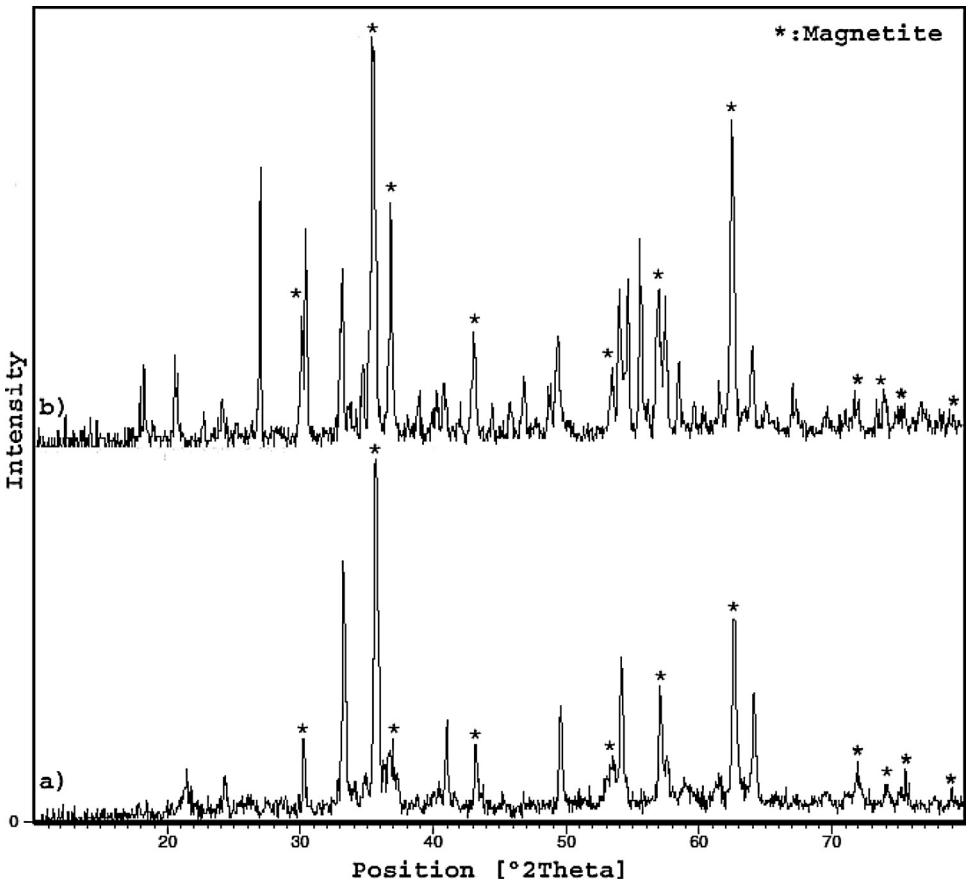

Fig. 2. XRD patterns of the synthesized samples at presence of different mineralizers: (a) S4, (b) S5.

the pure nanoscaled magnetite, the presence of both NaOH and $N_2H_4.H_2O$ is necessary.

At subsequent step, precursor effect was investigated. When $FeCl_2$ or $FeCl_3$ was used instead of $FeSO_4$, was produced the pure magnetite. But the prepared sample (S6) with precursor of $Fe_2(SO_4)_3$ was containing Fe_2O_3 and other impurities. For comparison, the XRD pattern of S6 is shown in Fig. 3. The studies were continued by changing $N_2H_4.H_2O$ with diamines of 1,2-phenylenediamine (PDA) and 1,8-naphthalenediamine (NDA). The pure magnetite was obtained with both diamines. For example, the XRD pattern of the prepared magnetite in presence of PDA (S9) is shown in Fig. 4. This diffraction pattern shows that the main peaks match to standard diffraction peaks of bulk material (Card No. 88-0315) and its characteristic peak with 100% intensity at $2\theta = 35.74^\circ$ is correspondence to the reflection plane (3 1 1). Respondent with index, Fe_3O_4 was identified by the diffraction peaks at 30.36°, 35.74°, 37.34°, 43.36°, 53.71°, 57.21°, 62.77°, 66.12°, 71.18°, 74.17° and 75.18°. These peaks indexed planes (2 2 0), (3 1 1), (2 2 2), (4 0 0), (4 2 2), (5 1 1), (4 4 0), (5 3 1), (6 2 0) (5 3 3) and (6 2 2) of the cubic magnetite with the crystallographical parameter of $a = 8.38$ Å. This pattern shows that the synthesized magnetite is completely pure.

Further information for the nanoscaled magnetite was obtained by scanning electron microscope (SEM). Fig. 5 shows SEM images of the prepared samples at presence of hydrazine (S3), PDA (S9) and NDA (S10) as reductant reagents. As can be observed, the spherical morphology for S3 (Fig. 5a and b) changed to nanosheet or aggregated nanoparticles morphologies in S9 (Fig. 5c and d) and S10 (Fig. 5e and f), respectively. In result, we selected the optimized conditions as S3.

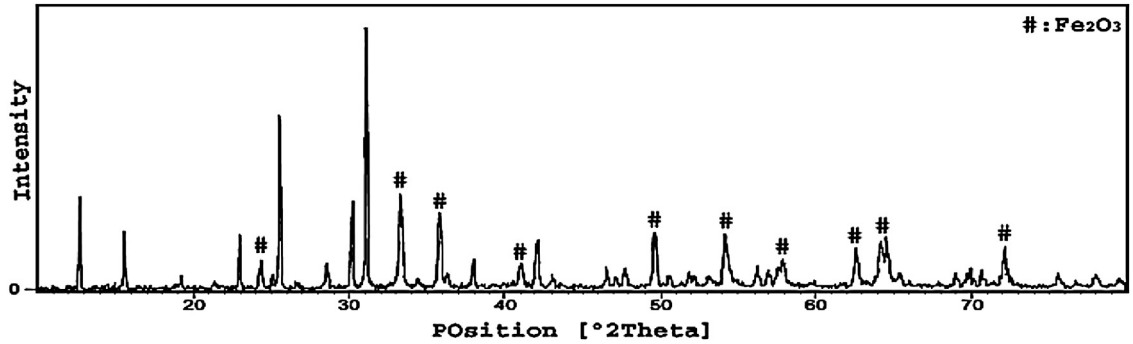

Fig. 3. XRD pattern of the prepared sample with $Fe_2(SO_4)_3$ (S6).

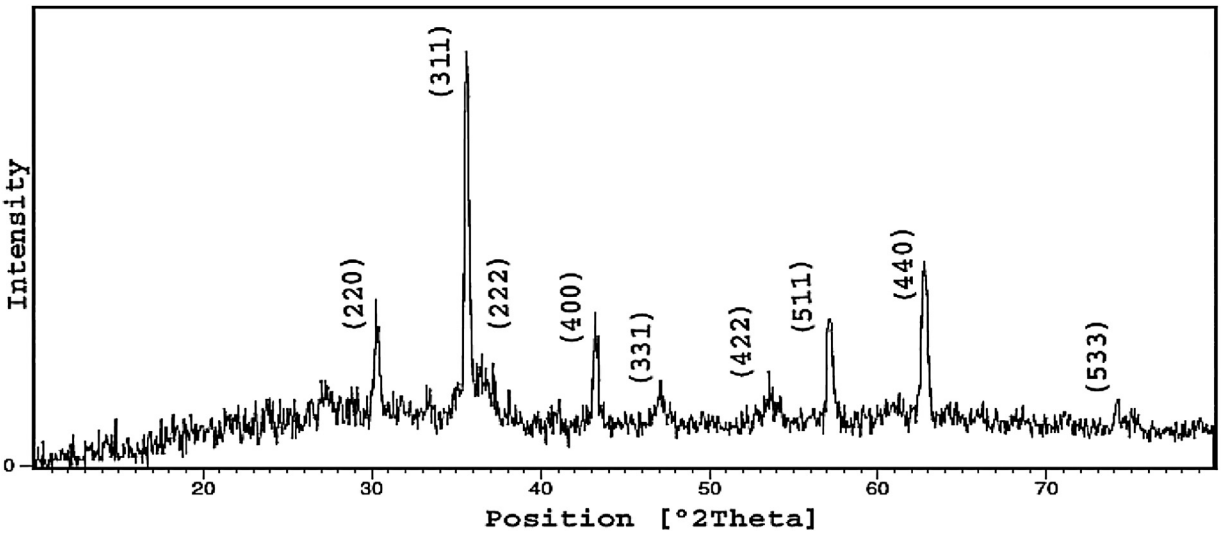

Fig. 4. XRD pattern of prepared magnetite sample with 1,2-phenylenediamine (S9).

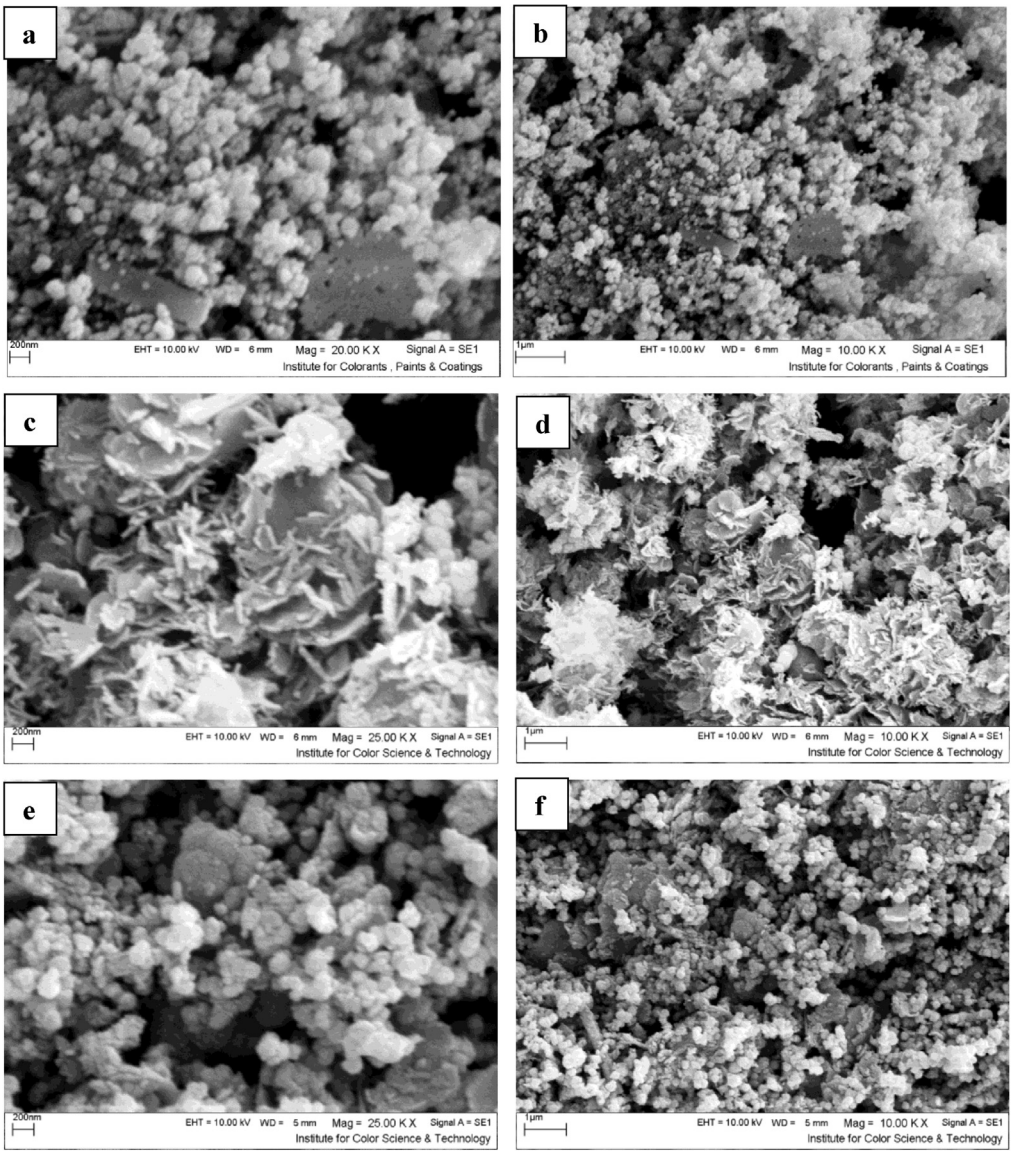

Fig. 5. SEM images of obtained magnetite products with various amines: (a, b) $N_2H_4.H_2O$ (S3), (c, d) PDA (S9), and (e, f) NDA (S10).

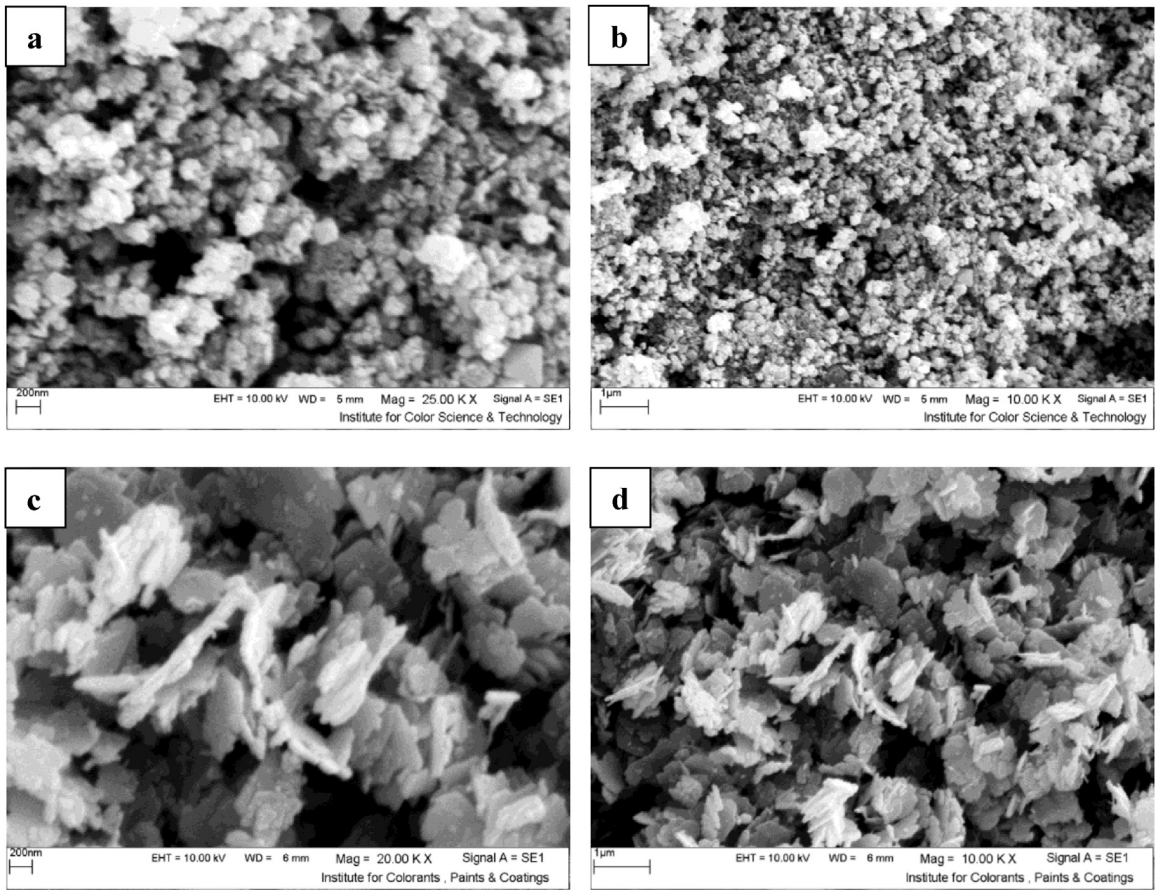

Fig. 6. SEM images of the synthesized magnetite products with the different precursors: (a, b) $FeCl_2$ (S7), (c, d) $FeCl_3$ (S8).

For further comparison, $FeCl_2$ and $FeCl_3$ are used as precursors. Fig. 6 shows the SEM images of S7 and S8 under the optimized conditions. The magnetite nanoparticles and nanosheets were formed using precursors of $FeCl_2$ and $FeCl_3$, respectively. Another effective reagent was solvent. Changing the solvent from water to ethanol leads to a slight agglomeration in the product (S11) (Fig. 7). As a result, the diamine, the solvent and precursor play important role on the morphology and structure of the synthesized magnetite.

Finally, a possible mechanism for the hydrothermal formation of the magnetite can be expressed as follow:

$$Fe^{2+} + 2OH^- \rightarrow Fe(OH)_2 \quad (1)$$

$$N_2H_4 + H_2O + 2e = 2NH_3 + 2OH^- \quad (2)$$

$$2Fe(OH)_2 + N_2H_4.H_2O \rightarrow 2Fe(OH)_3 + 2NH_3$$

or

$$2Fe^{2+} + N_2H_4.H_2O \rightarrow 2Fe^{3+} + 2NH_3 + 2OH^- \quad (3)$$

$$2Fe(OH)_3 + Fe(OH)_2 \rightarrow Fe_3O_4\downarrow + 4H_2O$$

or

$$2Fe^{3+} + Fe^{2+} + 8OH^- \rightarrow Fe_3O_4\downarrow + 4H_2O \quad (4)$$

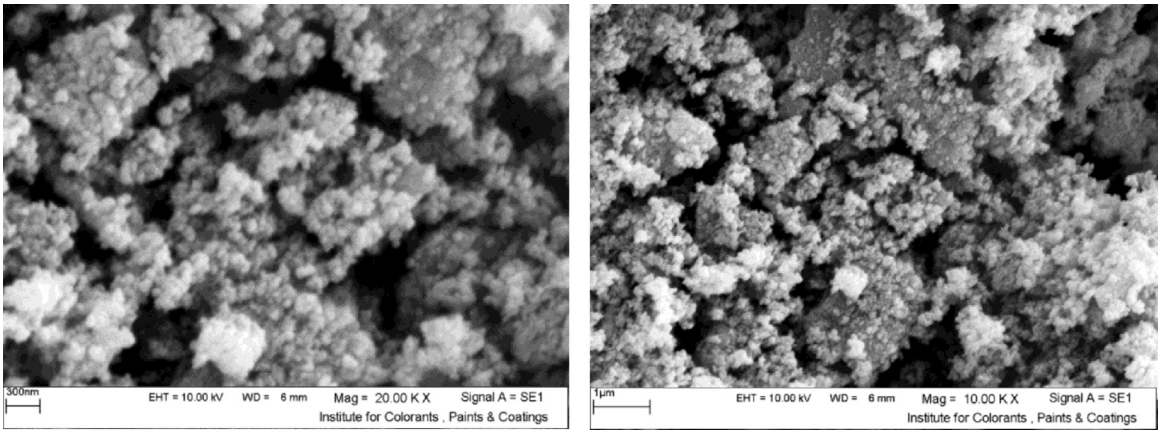

Fig. 7. SEM images of obtained magnetite with $N_2H_4.H_2O$ in ethanol (S11).

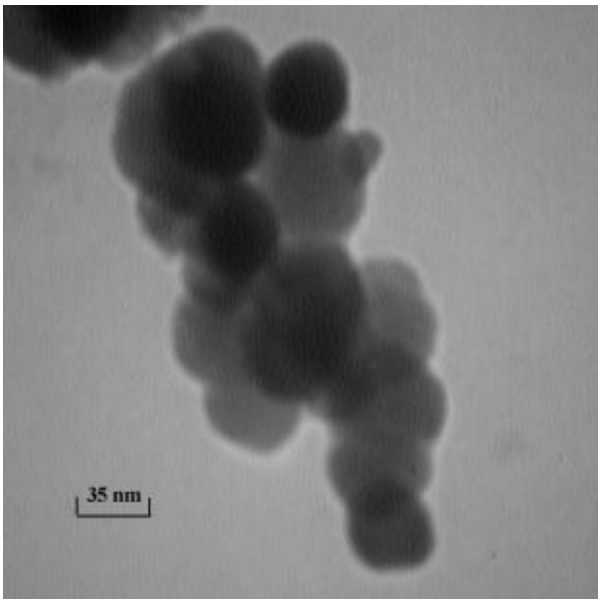

Fig. 8. TEM image of obtained magnetite with $N_2H_4.H_2O$ (S3).

Fig. 8 presents the TEM image of the synthesized sample of magnetite with $N_2H_4.H_2O$ (S3). This image shows that the magnetite has a spherical shape and its particles size is less than 100 nm. Furthermore, SEM images of the S3 (Fig. 5a and b) show that particles of the sample are uniform and in result we select this sample as a core for preparation of magnetite-porphyrin nanocomposite (MPNC).

The IR spectra of the synthesized magnetite nanoparticles, the magnetite coated with silica (Fe_3O_4/SiO_2) and the magnetite-porphyrin nanocomposite are shown in Fig. 9a. In the spectrum of magnetite nanoparticles is observed a broad band at ~3400 cm^{-1}, which is assigned to stretching vibrations of hydrogen bonding related to water molecules and hydroxyl groups of the magnetite. The strong band at 582 cm^{-1} is attributed to Fe–O vibration of Fe_3O_4 (Fig. 9a(i)). In the case of magnetite nanoparticles coated with silica, the sharp band at 1090 cm^{-1} is related to Si–O–Si antisymmetric stretching vibrations. This indicates existence of SiO_2 in the nanoparticles and the band at 3423 cm^{-1} is related to O–H stretching vibration of water. Fig. 9a(ii) shows the strong

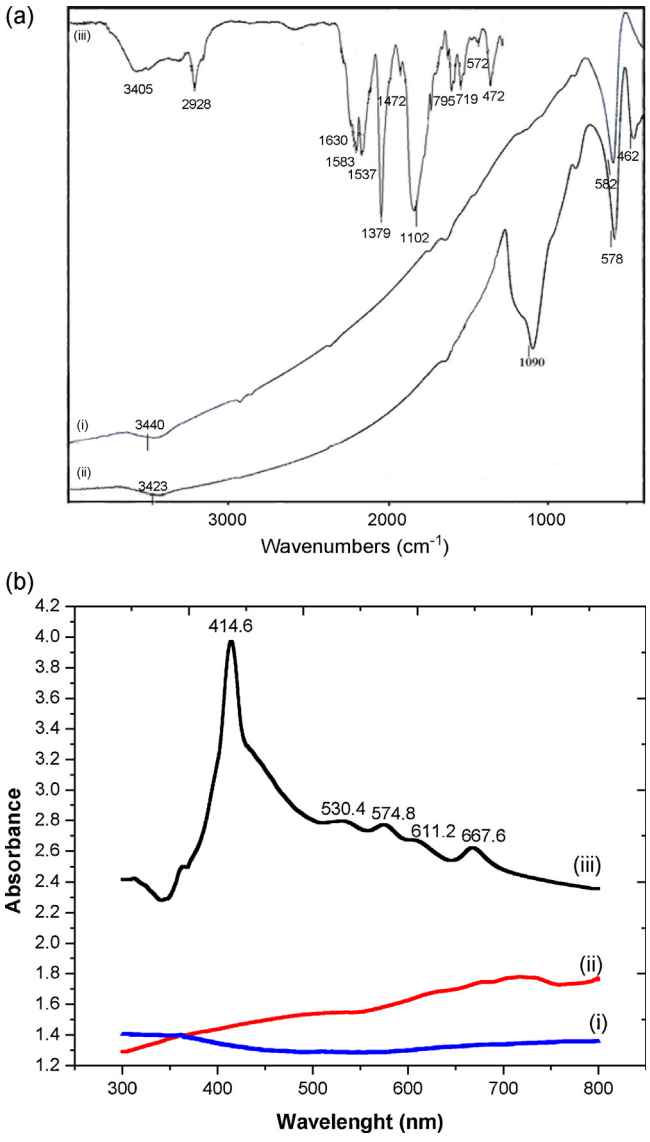

Fig. 9. (a) FT-IR spectra of magnetite nanoparticles (i), Fe_3O_4 nanoparticles coated with SiO_2 (ii), magnetite-porphyrin nanocomposite (iii). (b) DRS of magnetite nanoparticles (i) Fe_3O_4 nanoparticles coated with SiO_2 (ii), magnetite-porphyrin nanocomposite (iii).

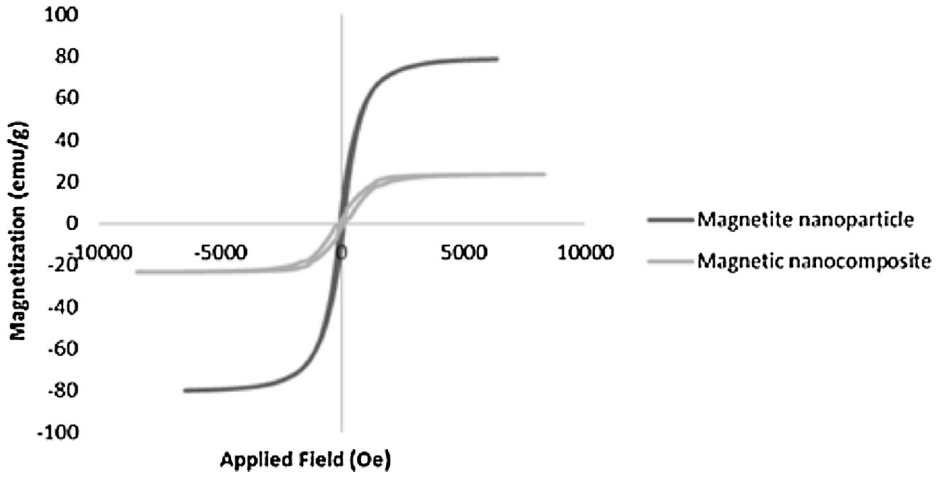

Fig. 10. Room temperature magnetization curve of magnetite nanoparticles and magnetite-porphyrin nanocomposite (MPNC).

absorption bands at 472 and 578 cm^{-1} related to Fe–O vibrations. FT-IR spectrum of the magnetite-porphyrin nanocomposite showed stretching vibrations for NH and CO (amide) related to amide groups of the porphyrin at 1472 and 1630 cm^{-1}. Other aromatic and aliphatic stretching vibrations of the porphyrin are found at 719, 795, 1583, 1537, 1379 and 2928 cm^{-1}. The presence of coated silica can be proved by strong bands at 1102 cm^{-1} (Fig. 9a(iii)).

The diffuse reflectance spectra (DRS) of the magnetic samples are shown in Fig. 9b. The DRS of Fe_3O_4 does not show any significant variation in the measured reflectance with visible and UV light. This is because of its band gap of about 0.1 eV [51]. Silica coating around the nanoparticles increases the relative amount of absorption without the appearance of a characteristic peak in the UV–vis range. The spectrum of the magnetite-porphyrin nanocomposite is quite similar to the UV–vis spectrum of porphyrin. This shows that the porphyrin is connected to the magnetite nanoparticle coated with silica (Fig. 9b(iii)).

The magnetite properties were studied using VSM at room temperature. Ferromagnetic behavior was observed with an S-Shaped hystersis loop, typical of magnetite. Fig. 10 shows the magnetization curve of the nanoscaled magnetite (S3) and the magnetite-porphyrin nanocomposite. The plot of the magnetization versus magnetic field (M-H loop) shows that the magnetite sample has strong magnetization and small coercivity (H_C). The saturation magnetization value (M_S) was calculated from VSM analysis, which is about 80 emu g^{-1} and is lower than the bulk magnetite (90–100 emu g^{-1}) [52]. As shown in Fig. 10, when applied magnetic field is removed, the synthesized nanoscaled Fe_3O_4 keeps very low remanence magnetic (M_R) ~ 8 emu g^{-1}. Coercivity value is low (~78 Oe) and indicates that the sample is soft magnetite material. Whereas (M_S), (M_R) and (H_C) values for the obtained magnetite-porphyrin nanocomposite were 23.5 emu g^{-1}, ~2 emu g^{-1}, ~82.5 Oe, respectively. The data show that the magnetite-porphyrin nanocomposite (MPNC) has magnetic property less than the magnetite nanoparticles, but is good candidate for removal of heavy cations from solutions by magnetic separation easily. After placing of a magnet besides the vial, materials was quickly attracted to the wall of the vial, Fig. 11.

Fig. 11. MPNC are attracted to the wall of the vial in presence of a magnet.

The adsorption of lead(II) ion with MPNC can be proved by XRD and EDS analysis. Fig. 12 shows the XRD patterns of the MPNC. This

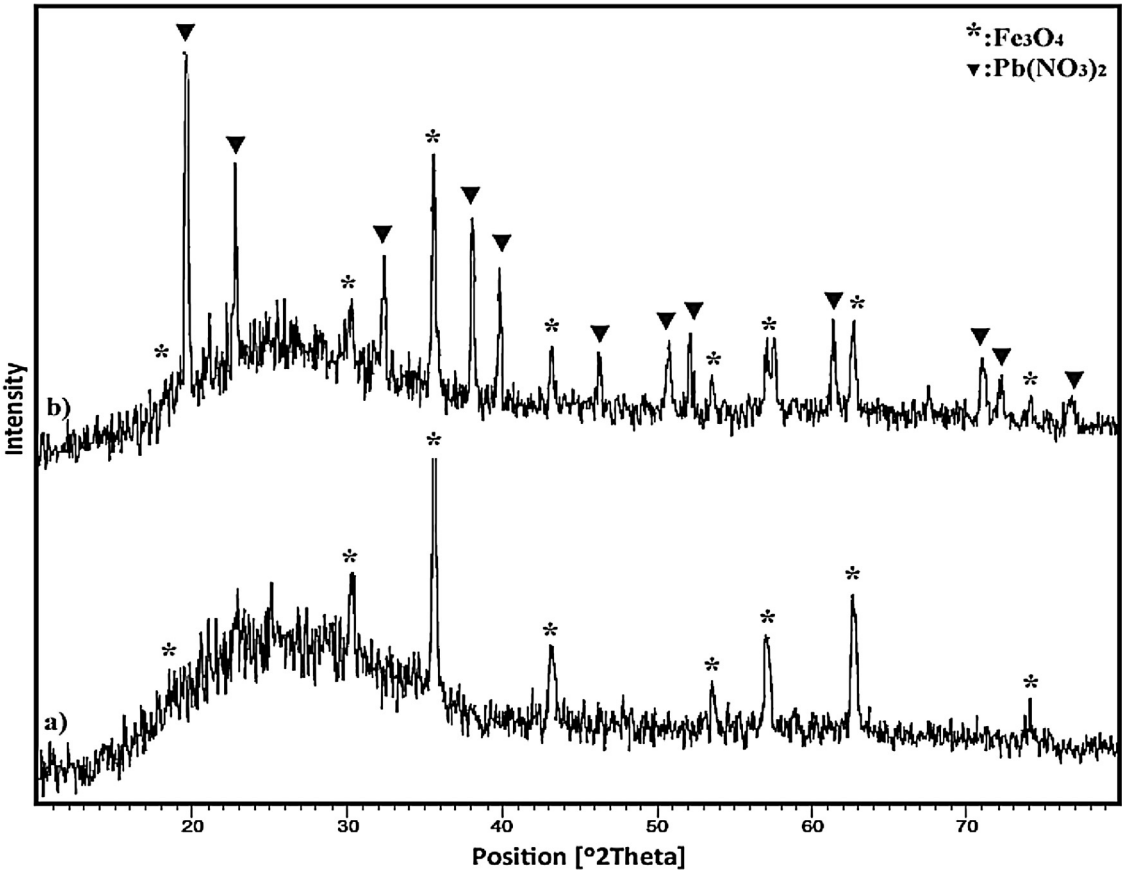

Fig. 12. XRD patterns of the magnetite-porphyrin nanocomposite (a) and the sample consist of MPNC and lead (b).

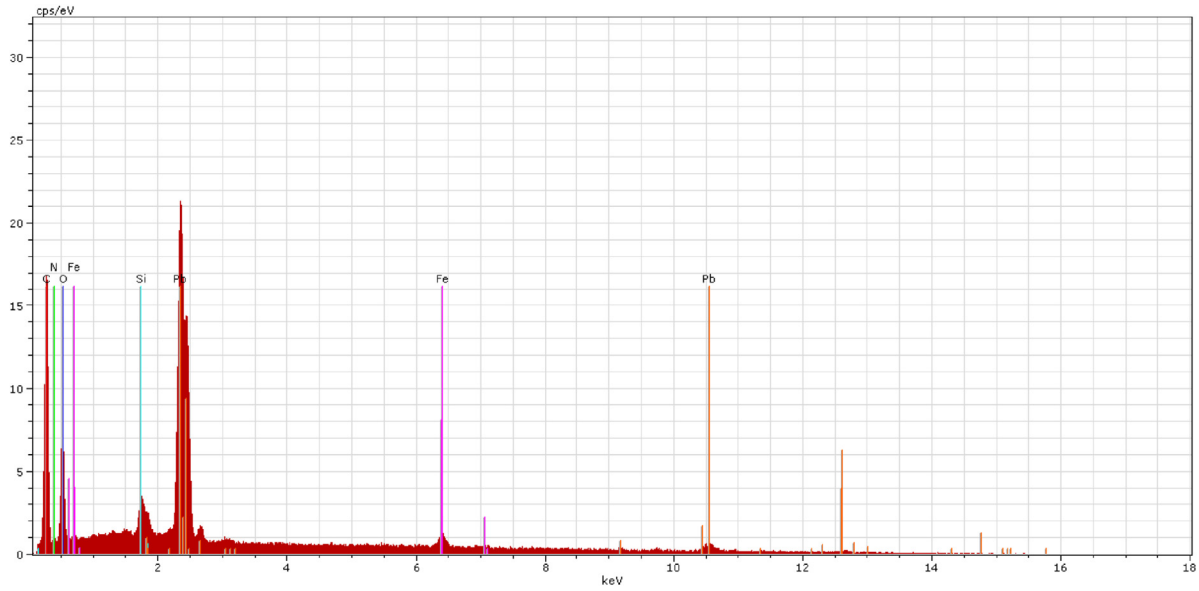

Fig. 13. EDS pattern of the sample consist of MPNC and lead.

figure shows that the sample contains both the magnetite related to MPNC and lead. Furthermore, the EDS pattern of this sample is containing MPNC and lead (Fig. 13).

The amount of lead ion adsorption by the magnetite sample was determined from a standard curve according to atomic absorption method. The data showed that the mass of lead that adsorbed by the magnetite sample was 2%. Also, the magnetite sample was not adsorbed cadmium or mercury ions from those solutions. As a result, with connection of the porphyrin to magnetite, adsorption of lead increases, and it enables us to remove cadmium and mercury ions from solutions. When the nanoparticles are modified to the nanocomposite, both qualitative and quantitative properties in removal of cations from water are improved. Furthermore, the amounts of lead and cadmium ions in the magnetite-porphyrin nanocomposite were determined from a standard curve according to atomic absorption method. Calculations showed that mass per cent lead and cadmium in the MPNC samples were 45.2% and 15.2%, respectively. The amount for mercury in the MPNC sample (with dithizone method) was mass 10%. In result, the MPNC acts as an effective material in removing heavy cations from water.

4. Conclusion

In summary, a simple hydrothermal method was used for preparation of nanoscaled magnetite powder in alkaline media. The results show that in this method, the pure nanosized magnetite is produced with cubic morphology. The prepared sample by reaction between $FeSO_4$ and hydrazinum hydrate was used for synthesis of magnetite-porphyrin nanocomposite. Also, the adsorption behavior of this magnetic nanocomposite for removing lead, cadmium and mercury ions was investigated. An important advantage for employment of the nanocomposite as adsorbent of heavy cations is simple separation by magnetic power. The results showed that the magnetite-porphyrin nanocomposite has the following advantages compared to the initial core: (1) Magnetite nanoparticles were only able to adsorption of lead ion, while the nanocomposite is can be adsorbed three ions (Pb^{2+}, Cd^{2+} and Hg^{2+}), (2) With modification of the magnetite to the nanocomposite, amount of the lead adsorption is increased from 2% to 45% that it is noteworthy. In a result, the synthesized nanocomposite removes heavy ion form water and so is separated from solution by a magnetic power easily.

Acknowledgements

The authors are grateful to University of Kashan for supporting this work by Grant No. (159183/8).

References

[1] J.M. Wood, Science 183 (1974) 1049–1052.
[2] Y. Mido, M. Satake, Chemicals in the Environment, Discovery Publishing House, New Delhi, 1995.
[3] K.M. Kadish, K.M. Smith, R. Guilard (Eds.), The Porphyrin Handbook, Academic Press, New York, 2000.
[4] R. Buntem, A. Intasiri, W. Lueangchaichaweng, J. Colloid Interface Sci. 347 (2010) 8–14.
[5] R.M. Cornell, U. Schwertmann, The Iron Oxides: Structures, Properties, Reactions, Occurences and Uses, Wiley-VCH, Weinheim, 2003.
[6] A.R. Lang, Dyes and Pigments: New Research, Nova Science Publishers, Inc, New York, 2009.
[7] R.M. Cornell, U. Schwertmann, Iron Oxides in the Laboratory, Wiley-VCH, Weinheim, 2000.
[8] M. Zhao, L. Josephson, Y. Tang, R. Weissleder, Angew. Chem. Int. Ed. 42 (2003) 1375–1378.
[9] L. Yang, X. Ren, F. Tang, L. Zhang, Biosens. Bioelect. 25 (2009) 889–895.
[10] B. Saha, S. Das, J. Saikia, G. Das, J. Phys. Chem. C. 115 (2011) 8024–8033.
[11] J.R. Sohn, J.S. Lim, Mater. Res. Bull. 41 (2006) 1225–1241.
[12] B.Z. Li, L. Wei, M. Gao, H. Lei, Adv. Mater. 17 (2005) 1001–1005.
[13] T.R. Sathe, A. Agrawal, S. Nie, Anal. Chem. 78 (2006) 5627–5632.
[14] K. Naka, A. Narita, H. Tanaka, Y. Chujo, M. Morita, T. Inubushi, I. Nishimura, J. Hiruta, H. Shibayama, M. Koga, S. Ishibashi, J. Seki, S.K. Kondoh, M. Hiraoka, Polym. Adv. Technol. 19 (2008) 1421–1429.
[15] S. Mornet, S. Vasseur, F. Grasset, P. Veverka, G. Goglio, A. Demourgues, J. Portier, E. Pollert, E. Duguet, Prog. Solid State Chem. 34 (2006) 237–247.
[16] L. Kong, X. Lu, X. Bian, W. Zhang, C. Wang, Appl. Mater. Interf. 3 (2011) 35–42.
[17] R. Aquino, F.A. Tourinho, R. Itri, M.C.F.L.E. Lara, J. Depeyrot, J. Magn. Magn. Mater. 252 (2002) 23–25.
[18] Z.Y. Zhong, T. Prozorov, I. Felner, A. Gedanken, J. Phys. Chem. B. 103 (1999) 947–956.
[19] D.E. Zhang, Z.W. Tong, S.Z. Li, X. Zhang, A. Ying, Mater. Lett. 62 (2008) 4053–4055.
[20] A.L. Morel, S.I. Nikitenko, K. Gionnet, A. Wattiaux, J.L.K. Him, C. Labrugere, B. Chevalier, G. Deleris, C. Petibois, A. Brisson, M. Simonoff, ACS Nano. 2 (2008) 847–856.
[21] R.A. Mukh-Qasem, A. Gedanken, J. Colloid Interface Sci. 284 (2005) 489–494.
[22] T. Sasaki, S. Ohara, T. Naka, J. Vejpravova, V. Sechovsky, M. Umetsu, S. Takami, B. Jeyadevan, T. Adschiri, J. Supercrit. Fluid. 53 (2010) 92–94.
[23] Z. Jing, S. Wu, Mater. Lett. 58 (2004) 3637–3640.
[24] H. Itoh, T. Sugimoto, J. Colloid Interface Sci. 265 (2003) 283–295.
[25] T. Sugimoto, K. Sakata, J. Colloid Interface Sci. 152 (1992) 587–590.
[26] M. Mohapatra, K. Rout, S. Anand, J. Hazard. Mater. 171 (2009) 417–423.

[27] K.A.M. Comb, D. Craw, A.J.M. Quillan, Langmuir 23 (2007) 12125–12130.
[28] C. Luengo, M. Brigante, J. Antelo, M. Aven, J. Colloid Interface Sci. 300 (2006) 511–518.
[29] E.A. Deliyanni, L. Nalbandian, K.A. Matis, J. Colloid Interface Sci. 302 (2006) 458–466.
[30] M. Mohapatra, S.K. Sahoo, S. Anand, R.P. Das, J. Colloid Interface Sci. 298 (2006) 6–12.
[31] A. Uheida, G. Salazar-Alvarez, E. Björkman, Z. Yu, M. Muhammed, J. Colloid Interface Sci. 298 (2006) 501–507.
[32] M.P. Morales, O.B. Miguel, R.P. Alejo, J.R. Cabello, S.V. Verdaguer, K. O'Grady, J. Magn. Magn. Mater. 266 (2003) 102–109.
[33] S. Guo, D. Li, L. Zhang, J. Li, E. Wang, Biomaterials 30 (2009) 1881–1889.
[34] C. Xu, B. Wang, S. Sun, J. Am. Chem. Soc. 131 (2009) 4216–4217.
[35] B. Xu, H. Dou, K. Tao, K. Sun, J. Ding, W. Shi, X. Guo, J. Li, D. Zhang, K. Sun, Langmuir 27 (2011) 12134–12142.
[36] J. Liang, Y. Xu, D. Sui, L. Zhang, Y. Huang, Y. Ma, F. Li, Y. Chen, J. Phys. Chem. C, 114 (2010) 17465–17471.
[37] Y. Li, H. Liao, Y. Qian, Mat. Res. Bull. 33 (1998) 841–844.
[38] M.T. Liang, S.H. Wang, Y.L. Chang, H.I. Hsiang, H.J. Huang, M.H. Tsai, W.C. Juan, S.F. Lu, Ceram. Inter. 36 (2010) 1131–1135.
[39] Q. Yitai, X. Yi, H. Chuan, L. Jing, C. Zuyao, Mater. Res. Bull. 29 (1994) 953–957.
[40] T.J. Daou, G. Pourroy, S. Be'gin-Colin, J.M. Grene'che, C. Ulhaq-Bouillet, P. Legare', P. Bernhardt, C. Leuvrey, G. Rogez, Chem. Mater. 18 (2006) 4399–4404.
[41] S. Giri, S. Samanta, S. Maji, S. Ganguli, A. Bhaumik, J. Magn. Magn. Mater. 285 (2005) 296–302.
[42] J. Wang, J. Sun, Q. Sun, Q. Chen, Mater. Res. Bull. 38 (2003) 1113–1118.
[43] Y. Zheng, Y. Cheng, F. Bao, Y. Wang, Mater. Res. Bull. 41 (2006) 525–529.
[44] N. Mizutani, T. Iwasaki, S. Watano, T. Yanagida, T. Kawai, Curr. Appl. Phys. 10 (2010) 801–806.
[45] H. Zhu, D. Yang, L. Zhu, Surf. Coat. Tech. 201 (2007) 5870–5874.
[46] Q. Chang, L. Zhu, C. Yu, H. Tang, J. Lumin. 128 (2008) 1890–1895.
[47] A.M.R. Gonsalves, J.M.T.B. Varejão, M.M. Pereira, J. Heterocycl. Chem. 28 (1991) 635–640.
[48] H. Imahori, J.C. Liu, H. Hotta, A. Kira, T. Umeyama, Y. Matano, G. Li, S. Ye, M. Isosomppi, N.V. Tkachenko, H. Lemmetyinen, J. Phys. Chem. B. 109 (2005) 18465–18474.
[49] M. Nowostawska, S.A. Corr, S.J. Byrne, J. Conroy, Y. Volkov, Y.K. Gun'ko, J. Nanobiotech. 9 (2011) 13–24.
[50] M.C. Rand, A.E. Green Berg, M.J. Taras, Standard Methods for the Examination of Water and Wastewater (APHA-AWWA-WPCF-14 Edition) Washington, 1975, pp. 229–231.
[51] Y. Xu, M.A.A. Schoonen, Am. Min. 85 (2000) 543–556.
[52] D.H. Han, J.P. Wang, H.L. Luo, J. Magn. Magn. Mater. 136 (1994) 176–182.